Study of pedestrians' mixed thermal responses when experiencing rapid and simultaneous variations in sun and wind conditions in urban continuums

Jianong Li, Jianlei Niu*, Cheuk Ming Mak

Department of Building Environment and Energy Engineering, The Hong Kong Polytechnic University, Hunghom, Kowloon, Hong Kong

Abstract

Rich, rapid, and simultaneous variations in wind and solar radiation produced by complex urban continuums are supposed to have positive effects on thermal comfort during walking. However, the identification of these influences is still challenging. In view of this, this study observed the mixed thermal perceptions and skin temperature of 70 healthy young college students when strolling in two complex urban continuums and experiencing rapid variations in sun and wind conditions. An index was proposed to categorize the varying wind and solar radiation in both numerical and geometrical respects. The results showed that, the intensities of varying wind, varying solar radiation, and air temperature simultaneously influenced the mixed thermal perceptions. Meanwhile, the intensity of simultaneously varied wind and solar radiation can be quantified by the mean skin temperature variability in a multiple linear model. An increase in the intensity of simultaneously varied wind and solar radiation led to a two-degree rise in the acceptable air temperature and a 1.2-degree increase in the mean skin temperature threshold for irritation. The study revealed the effects of simultaneously varied wind and solar radiation on pedestrian thermal comfort, motivating urban planners to take advantage of the dynamic nature created by urban morphologies to generate wind and solar radiation variations for comfort.

Key words: Dynamic thermal environment; Walking; Urban continuum; Variations in wind and solar radiation; Skin temperature; Thermal comfort

1. Introduction

The frequent occurrence of heat waves in recent years, especially in 2022, discourages outdoor activities and increases the related health risk (WHO, 2018; WMO, 2022), bringing negative influences on citizens' daily life. However, outdoor activities such as walking, sitting and biking in urban areas are inevitable in the daily life and essential for the physical and mental health (Asimakopoulos et al., 2012). In addition to the worldwide control of the global warming, initiatives to improve thermal conditions in densely populated urban regions, such as business district streets, community living circles, and campus where walking is the most prevalent outdoor activities, are of critical relevance. In view of this, it is urgent to examine the thermal comfort of pedestrians walking in such localized urban regions in order to develop novel solutions for improving thermal conditions.

Urban areas are characterized with complex building blocks and vegetation, and solar radiation and air flow are easily altered by urban designs, resulting in a diversity of microclimate environments and outdoor thermal comfort in urban continuums (Ahmed-Ouameur et al., 2007; Li et al., 2020; Vasilikou et al., 2020; Xie et al., 2018; Yang et al., 2013). Therefore, encountering rapid and constant variations in wind and solar radiation when walking in a localized urban area should be fairly typical. Previous studies have examined the cooling effects of wind turbulence on thermal comfort in warm-biased indoor environments (Cao et al., 2021; Huang et al., 2012; Ouyang et al., 2006; Xia et al., 2000), the impact of a single step change in solar radiation on thermal load (Hodder et al., 2007; Lai et al., 2017; Shimazaki et al., 2011; Zhou et al., 2020), and the impact of a single step change in air temperature on transient thermal comfort (De Dear et al., 1993; Fiala, 1998; Frank et al., 1999; Guan et al., 2003; Kingma et al.,

2014; Takada et al., 2009; Zhang, 2003). However, these studies were all conducted with people seated or standing, and there is a lack of study on the combined effects of rapidly varying wind and solar radiation encountered during walking on thermal comfort. Overlooking the impacts of these rapid and constant variations in wind and solar radiaiton might be the reason leading to a less accurate prediction of pedestrains' thermal comfort in previous studies (Li et al., 2022; Xie et al., 2018; Yu et al., 2020).

According to previous studies, a transient or dynamic thermal environment may promote a possible state of 'mixed' perception when internally born 'warnings of hot' from raised central temperature are relieved by 'warnings of cool' from thermo-receptors (Ahmed-Ouameur et al., 2007; Fiala et al., 2001), or an "alliesthesia" phenomenon with a pleasant or annoyed perception ahead of the thermo-regulation responses (de Dear, 2011; Lai et al., 2020; Liu et al., 2021). These phenomena are helpful for improving thermal satisfaction in both indoor and outdoor environments, and it is hypothesized that the appropriate utilization of varying wind and solar radiation created by walking in urban continuums could also improve the thermal satisfaction during walking (Cao et al., 2021; Li et al., 2022; Zhang et al., 2009). In light of previous research, investigating pedestrians' mixed thermal perceptions during walking and assessing the influences of simultaneously varying wind and solar radiation encountered during walking are a major challenge for this study.

To overcome the challenges, this study firstly aims to quantify the intensity of variations in wind and solar radiation. On the basis of previous findings that the skin temperature variation followed the pattern of air movement or solar radiation (Parkinson et al., 2016; Yu et al., 2021; Zhou et al., 2020), it is anticipated that the feature of simultaneously varying wind and solar radiation can be equivalent to the variability of skin temperature other than the change rate of

skin temperature. And then, if a rise in the intensity of simultaneous variations leads to an increase in the tolerance for high temperatures will be explored to identify the favorable influences of varying wind and solar radiation. The study is expected to firstly give a knowledge of how simultaneously varying wind and solar radiation encountered during walking affect pedestrian thermal comfort in the real scenario and to highlight the need for improvement of researches on assessing dynamic thermal comfort. Given the knowledge, it aims to disseminate the concept of taking advantage of the complexity in urban areas, which is produced by spatiotemporal distributions of buildings and artificial devices, to create appropriate variations in wind and solar radiation for improving thermal comfort, rather than taking great efforts and expense to directly lower air temperature.

2 Methodology

2.1 Experiment design

2.1.1 Site and date

The simultaneous variations in wind and solar radiation were experienced by pedestrians strolling in the densely populated urban continuums with a variety of building blocks. Two urban continuums were selected to conduct the experiments; one is a university campus and the other consists of urban streets. Figure 1a shows district plans of two experiment sites and selected pedestrian routes during experiments. Experiments were conducted in hot-humid subtropical Hong Kong from late July to early October, 2020, during which the overall climate conditions are summarized in Table 1 (HKO, 2020)

Table 1 Summary of climate conditions of Hong Kong during the experiment periods

Month	Mean	Air Temperature	Mean	Total	Prevailing	Mean

4

	Pressure (hPa)	Mean Daily Max (°C)	Mean (°C)	Mean Daily Min (°C)	Relative Humidity (%)	Bright Sunshine (hours)	Wind Direction (degrees)	Wind Speed (km/h)
07	1007.4	32.7	29.8	27.7	78	249.7	180	9.4
08	1006.4	31.6	28.6	26.3	82	195.7	110	8.6
09	1008.9	30.8	28.0	26.0	84	131.3	100	8.7
10	1012.9	27.7	25.0	23.1	70	190.9	090	12.4

2.1.2 Subject and activities

70 college students, including 32 males and 38 females aged 21 to 30, were recruited as subjects to participate in the experiments, and the duration of each experiment was controlled within 90 minutes. Female subjects have an average height of 160.6±3.1 cm and an average weight of 49.5±5.3 kg, while male students have an average height of 175.8±2.6 cm and an average weight of 63.2±3.6 kg. One or two subjects walked on the designated route in each experiment, and they were required to wear short-sleeved T-shirts, short trousers, and sports shoes with a general clothing insulation of 0.3-0.4 clo (ASHRAE, 2013a; ISO, 2005).

There were two stages in each experiment: stage 1, the preparation stage in a shaded area, in which subjects sit on a chair for 30 minutes being introduced by the experiment procedure and being attached skin temperature sensors; stage 2, the walking stage, in which subjects will walk and rest for four times while encountering varying wind and solar radiation and being asked about their transient thermal perceptions; each walking period lasts about 5 to 10 minutes. Figure 1b and Figure 1c depict the experiment procedures in two experiment sites, illustrating a variety of urban forms and microclimate environments passing by.
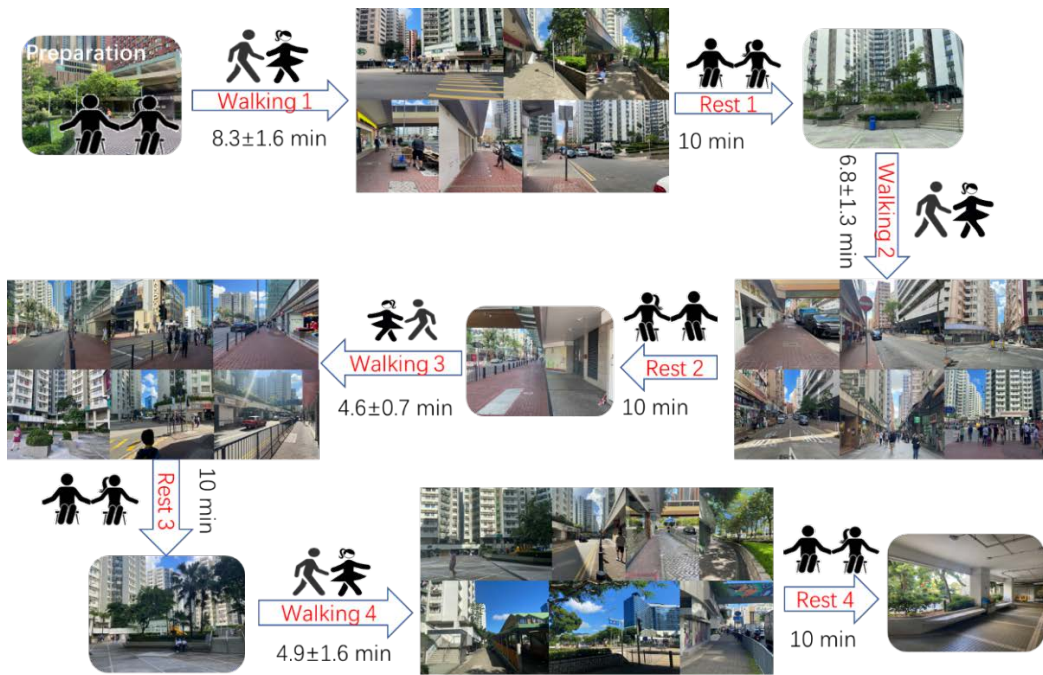
Table. 2 summarizes the experiment date, daily air temperature, subjects' information, initial thermal conditions at stage 1, and information of walking periods on campus and in the urban street. The building or green density in Table 2 is defined by the ratio of building area or green area to the total area of an experiment continuum, and the metabolic rates during walking were determined by average walking speed based on 2017 ASHRAE fundamentals (ASHRAE, 2017). Affected by the experiment time, 10:00-12:00 in the morning and 14:30-16:30 in the afternoon, and walking direction from North (North-West) to South (South-East) during experiments, sunshine was almost at the front and side of a subject's body, which makes sure that subjects can fully feel the changes in sunshine.

- Blue Line—Walking period 1
- Red Line—Walking period 2
- Yellow Line—Walking period 3
- Purple Line—Walking period 4

a)

b)

c)

Figure 1 Information of experiments: a) District plans on campus and urban streets; b) Subjects activities on campus; c) Subjects activities in the urban streets.

Table 2 Experiment date, daily air temperature, subjects' information, and initial thermal conditions at stage 1, and information of walking periods on campus and in the urban street

Area	Experiment time	Experiment date	Daily Air temperature (min-max)	Gender (F: Female M: Male)	Average age (Year)	T_a (°C)	RH (%)	T_g (°C)	v (m/s)	Duration (min)	Distance (m)	Speed (m/min)	Metabolic rate (MET)
				Information of subjects		Initial thermal condition at stage 1				Information of each walking period (Average)			
2.3Campus Les2.3s Crowded Noise Decibel: 64dBA Building density (0.34) Green density (0.13)	AM 10:00-12:00	7/21	28.1-34.7	2 M	25	29.4	64.8	29.7	1.2	8	430	54	2.1
		7/29	28.6-34.9	2 M	25	29.3	73.8	30.6	1.4	7	430	61	2.3
		8/8	28.4-34.4	2 M	23	30.3	67.5	30.5	1.3	6	430	71	2.5
		8/15	27.9-33.0	1 F	28	29.2	70.1	30.1	1.0	6	430	71	2.5
		8/18	25.6-29.9	2 M	24	28.5	73.2	29.7	1.2	6	430	71	2.5
		9/12	26.2-32.4	2 M	22	30.7	69.0	32.2	1.6	8	430	54	2.1
		9/21	25.5-29.7	1 M	19	28.6	81.1	28.8	1.5	6	430	71	2.5
		9/22	26.6-31.4	1 F	21	29.0	73.0	29.9	1.0	6	430	71	2.5
		9/24	27.1-31.3	1 F/ 1 M	22	27.8	76.1	29.2	1.2	6	430	71	2.5
		9/25	26.6-31.4	2 F	26	28.4	69.8	28.7	0.9	6	430	71	2.5
		9/26	27.1-29.7	2 F	26	28.1	72.8	28.7	1.4	7	430	61	2.3
	PM 14:30-16:30	7/27	28.4-33.5	2 M	25	30.9	63.7	30.9	0.5	6	430	71	2.5
		7/29	28.6-34.9	1 M	25	31.8	65.4	32.6	0.9	7	430	61	2.3
		7/30	26.0-34.9	1 F	25	30.7	64.8	30.7	1.1	7	430	61	2.3
		8/5	26.0-34.9	1 F	25	29.8	76.4	29.9	1.1	7	430	61	2.3
		8/8	28.4-34.4	1 M	23	31.9	65.0	33.1	1.4	6	430	71	2.5

		8/10	28.3-33.0	1 F	22	30.1	68.4	30.5	1.2	6	430	71	2.5
		8/20	27.2-32.2	2 F	27	28.4	73.0	30.5	1.1	7	430	61	2.3
		9/18	26.4-30.2	2 M	22	29.0	71.2	30.2	1.8	7	430	61	2.3
		9/23	27.4-31.9	1 M	22	30.1	69.3	31.0	1.1	6	430	71	2.5
		9/26	27.1-29.7	1 F / 1 M	22	28.5	69.0	28.8	1.1	6	430	71	2.5
		10/3	26.7-31.9	1 F	22	29.6	62.0	30.6	1.6	6	430	71	2.5
Urban streets Crowded Noise Decibel: 68dBA Building density (0.49) Green density (0.02)	AM 10:00-12:00	8/28	25.0-34.2	2 M	26	30.9	72.0	32.6	0.6	7	450	61	2.3
		9/4	28.2-34.3	2 F	26	30.2	76.0	31.3	0.6	9	450	50	2.1
		9/16	27.3-32.9	2 M	22	30.5	75.3	31.3	0.4	8	450	56	2.1
		9/23	27.4-31.9	2 F	26	30.1	68.6	32.1	0.9	7	450	61	2.3
		9/26	26.2-29.4	2 F	25	28.3	75.0	30.5	1.8	7	450	61	2.3
		10/3	26.7-31.9	1 F / 1 M	22	28.7	69.8	30.6	1.4	7	450	61	2.3
		10/4	26.8-31.4	2 M	21	29.9	66.4	32.4	0.8	7	450	61	2.3
		8/22	27.2-33.3	2 M	28	31.9	61.8	33.5	0.8	7	450	61	2.3
		8/29	27.8-33.2	1 F / 1 M	29	31.4	68.9	32.5	0.7	8	450	56	2.1
		8/31	28.2-34.3	2 M	29	31.0	64.3	31.0	1.0	8	450	56	2.1
	PM 14:30-17:00	9/5	25.2-30.6	1 F / 1 M	28	30.5	68.0	33.0	0.5	7	450	61	2.3
		9/6	27.2-32.3	2 M	25	30.1	72.9	32.5	0.7	8	450	56	2.1
		9/7	26.8-33.3	2 F	25	31.1	70.5	33.4	1.2	7	450	61	2.3
		9/16	27.3-32.9	1 F / 1 M	22	31.1	72.1	32.6	1.2	8	450	56	2.1
		9/22	26.6-31.4	2 F	23	30.2	69.0	32.6	0.9	8	450	56	2.1
		9/24	27.1-31.3	2 F	22	29.9	73.9	30.4	1.2	7	450	61	2.3

2.1.3 Questionnaire survey

To explore "mixed" thermal perceptions during walking, the questionnaire designed in this study consisted of three questions (Figure 2a): 1, the ASHRAE 7-point Thermal Sensation Vote (*TSV*); 2, the Thermal Pleasure (*TP*); and 3, the Need for changing temperature/solar/wind conditions (*N*). In each walking period, subjects were required to answer questions 1 and 2 when experiencing changes in sunlight, shade, and wind to record their transient perceptions (*TSVt* & *TPt*) of varying sun and wind conditions.

Question 3 was designed to describe the subjects' need for reducing solar radiation, increasing air movement and cooling. The answer to question 3 has 6 scales ranging from 0 to 5, with 0 reflecting no need to 5 reflecting an extremely strong need to change the current microclimate states, and subjects were required to answer question 3 every 2 minutes during walking. The artificial intelligence (AI) recorder shown in Figure 2b was used for recording subjects' answers. Recordings were then transferred to words with the software after each experiment.

a)

Sougo AI Recorder   Software for transcription

b)

Figure 2 Questionnaire survey: a) Questionnaire; b) AI recorder and transcription software for collecting answers to the questionnaire

2.2 Measurements and calculations

2.2.1 Meteorological parameters

During the experiments, the meteorological parameters were measured and collected by a movable weather station all the time (Figure 3). All instruments for measuring meteorological parameters were mounted on a baby carriage for shock absorption, which was wheeled alongside the subjects at a consistent space for measuring air temperature (T_a), wind speed (v), relative humidity (RH), and global temperature (T_g) at pedestrian level, and the data was recorded at a 1s interval. The specifications of the equipment are displayed in Table 3. The mean radiant temperature T_{mrt} calculated from T_g was adjusted through calibration with three Kipp & Zonen CNR4 net radiometers using equation (1) (Li et al., 2022), and T_{mrt} in this study was used to reflect the solar radiation received by subjects. The system time of all instruments was calibrated to local time before the experiment.

$$T_{mrt(Tg)} = 1.1383 \times T_{mrt(6-direction)} - 3.6986 \qquad (1)$$

where, $T_{mrt(6-direction)}$ represents the T_{mrt} calculated from six directions' radiation from three Kipp & Zonen CNR4 net radiometers; $T_{mrt(Tg)}$ represents the T_{mrt} calculated from T_g.
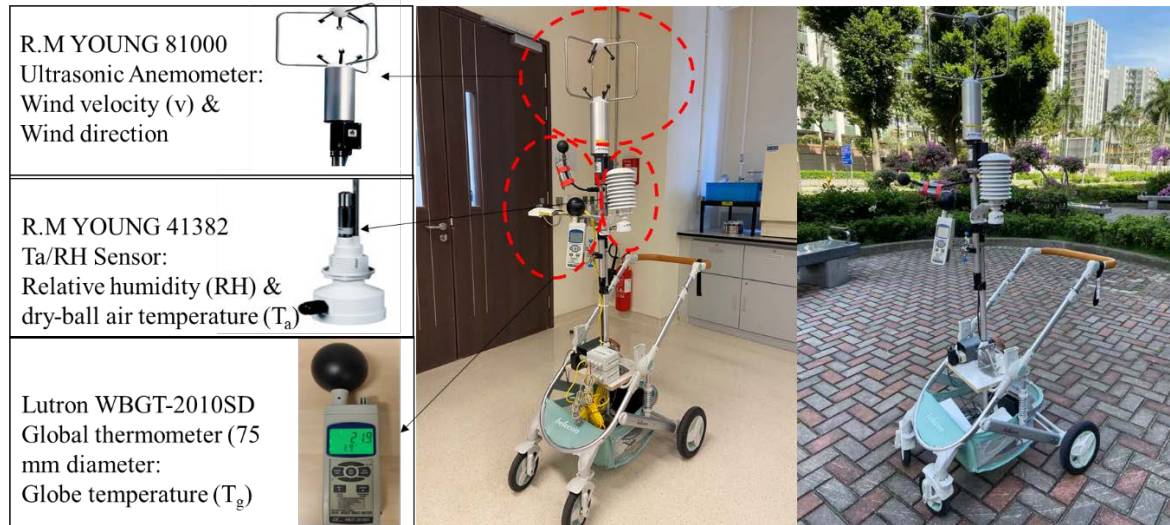

Figure 3 Movable mini weather station: a) equipment pictures; b) equipment specifications

Table 3 Equipment specifications

Meteorological parameter	Instrument	Measuring Range	Accuracy
Air temperature	R.M.YOUNG 41382	-50-50 ℃	±0.3 ℃
Relative humidity		0-100%	±1%
Wind speed	R.M.YOUNG 81000	0-40 m/s	±0.05 m/s
Globe temperature	Lutron WBGT-2010SD	0-80 ℃	±0.6 ℃

It should be noted, however, that according to the contents in Appendix A, it took at least two minutes for T_g to reach stable while switching between sunlight and shade. Considering the relatively fast and various switches between sunlight and tree-shade and between sunlight and building-shade (UEB in Appendix A) in this study, 2 minutes was thus taken as the minimum stabilized time of T_g after one step change. In light of this, the measured globe temperature during movement was adjusted based on the following assumption to simplify the analysis.

On sunny days, if walking in the shade from sunlight lasted more than 2 minutes, the global temperatures in the first two minutes after entering the shade were approximated using the globe temperature at 2 minutes instead. If the time spent in the shade was less than 2 minutes, the globe temperature in the shade was approximated using the globe temperature measured right before re-entering the sunlight. A similar assumption was adopted for adjusting the globe temperature measured when walking in the sunlight. On cloudy days, there were no intense changes in solar radiation, and the measured globe temperatures during walking were not adjusted.

2.2.2 Local skin temperature

In this study, we measured 12 points of skin temperature with small and portable thermocouples called the i-Button temperature sensor (Figure 4). The measured skin temperatures were automatically recorded in the i-Button itself, at a 3 s interval. Before the measurements, all the i-Button temperature recorders were calibrated against a standard mercury thermometer with a precision of 0.1 °C. The mean skin temperature (*MST*) was calculated using the 9 points local skin temperatures recommended by Houdas and Colin et al. (Houdas et al., 1982; Liu et al., 2011), which took the cheek temperature into account while calculating the mean skin temperature. The weighting method (Eq. 2) was used and the weighting factors of points are reported in Table 4.

$$MST = \sum_{i=1}^{n} k_i T_i \quad (2)$$

where T_i is local skin temperature, k_i is the corresponding weighting factor and n is the number of measuring sites.

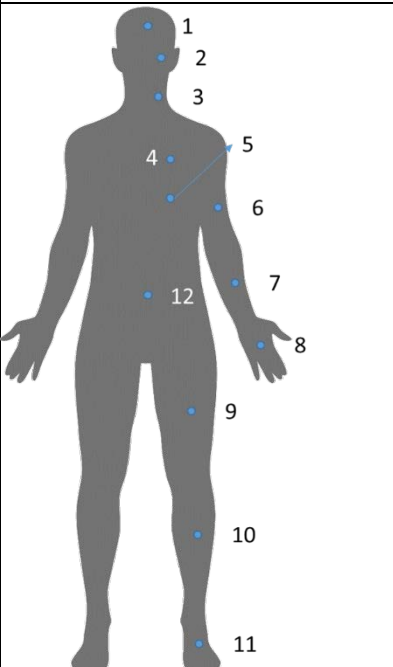Table 4. Measurement sites and corresponding weighting factors.

		Weighting factors of points
		Houdas & Colins et al.
	1 Forehead	
	2 Cheek	0.20
	3 Neck	
	4 Chest	0.05
	5 Back	0.20
	6 Upper arm	0.10
	7 Forearm	0.05
	8 Hand	
	9 Thigh	0.125
	10 Leg	0.075
	11 Foot	0.075
	12 Abdomen	0.125

Figure 4 Thermocouples (i-Button) for measuring skin temperature.

2.3 Proposed indices

2.3.1 Sensed Variation Index

As introduced in Section 2.1.3, subjects were required to answer questionnaires when experiencing changes in sunlight, shade, and wind during walking. Therefore, wind speed and

mean radiant temperature corresponding to transient answers were extracted to study their sensed variations in urban continuums. Because the single coefficient of variation (ratio of standard deviation to mean) is insufficient to describe the variation, a new index that describes the variation in both quantitative and geometric aspects has been developed based on the Mei-Wang fluctuation (*MWF*) index applied in hydro-wind systems (Wang et al., 2016). The new index is called the Sensed Variation Index (*SVI*), and it integrates the coefficient of variation and change rate of extracted wind speed and mean radiant temperature in each walking period. The calculation of *SVI* can be visualized in Figure 5.
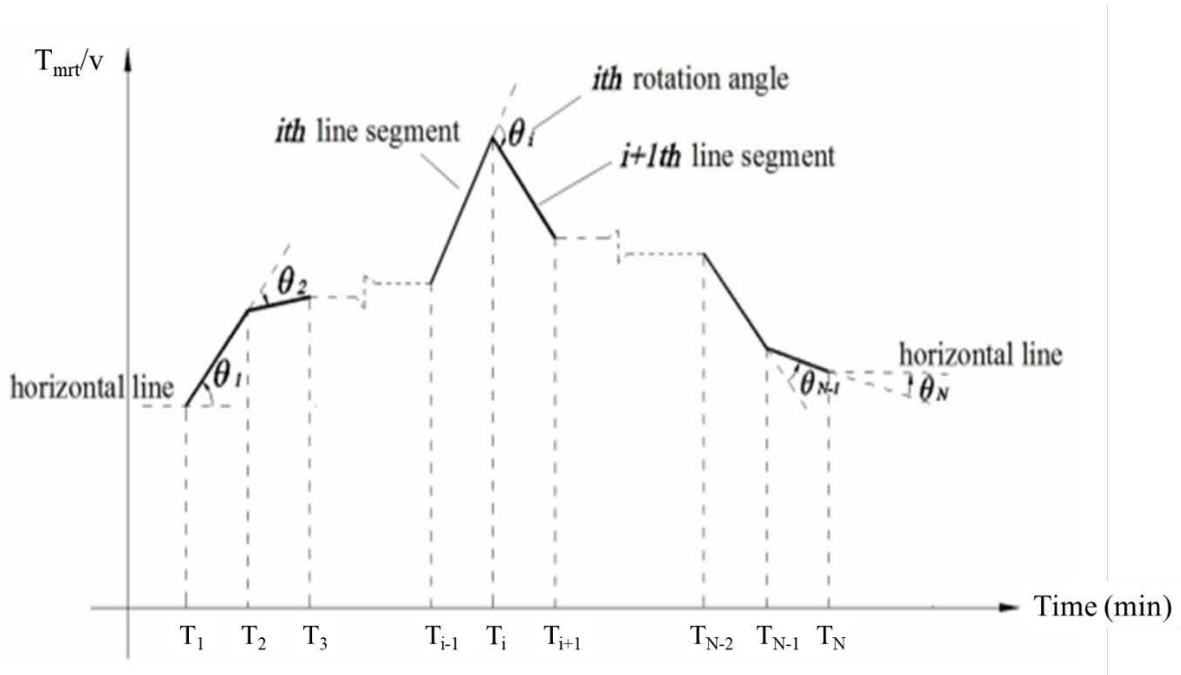
Figure 5 Diagram of rotation angle and line segment of a parameter's variation: The abscissa shows the total time for one walking period, and T_i shows the time corresponding to the ith question answer. The ordinate shows the value of T_{mrt} or *v*.

The coefficient of variation (*cv*) expressed as Eq. (3) is a standardized measure of frequency distribution dispersion, which is used to describe the quantitative variations of wind speed or mean radiant temperature during walking.

$$cv = \frac{\sqrt{\frac{1}{N}\sum_{i=1}^{N}(y(i)-\bar{y})^2}}{\bar{y}} \qquad (3)$$

where y(*i*) is the ordinate of the T_{mrt} or *v* corresponding to the transient answer as a polyline in the rectangular coordinate system; *i* is the ith question answered in a walking period; the time interval between *i* and *i*+1 is the duration of a sequential answer; *N* is the total number of questionnaire surveys in a walking period; $\bar{y}$ is the mean of the y(*i*) values; and *cv* is the coefficient of variation of T_{mrt} or *v*.

The change rate in T_{mrt} or *v* was derived from the rotation angle rate that can be determined using equations (4-6):

$$\alpha = \frac{\sum_{i=1}^{N}\theta_i}{T} \; (°/min) \qquad (4)$$

$$\theta_i = \begin{cases} arctan|k_i| & i = 1 \; or \; N \\ |arctank_i - arctank_{i-1}| & 2 \leq i \leq N-1, and \; k_i \times k_{i-1} \geq 0 \\ arctan|k_i| + arctan|k_{i-1}| & 2 \leq i \leq N-1, and \; k_i \times k_{i-1} < 0 \end{cases} \qquad (5)$$

$$k_i = \begin{cases} \frac{y(i+1)-y(i)}{T(i+1)-T(i)} & 1 \leq i \leq N-1 \\ \frac{y(N)-y(N-1)}{T(N)-T(N-1)} & i = N \end{cases} \qquad (6)$$

where *T* in minutes is the total period for one walking; θ_i is the rotation angle for one change in a parameter, as shown in Figure 5. When $2 \leq i \leq N-1$, θ_i is the degree of rotation between two adjacent change line segments, while when *i* = 1 or N, it is the acute angle formed by the first or Nth line segment and a horizontal line. When $1 \leq i \leq N-1$, k_i is the slope of the ith line

segment; in another word, the change rate between i^{th} parameter value and $(i-1)^{th}$ parameter value; while when $i = N$, it is the slope of $(N-1)^{th}$ line segment. The symbol α represents the degree or level of the shape variation of a parameter. As a result, Eq. (7) can define the variation of a parameter in both quantitative and shape aspects in each walking period, and the larger the *SVI* value, the more intense the variation of T_{mrt} or v felt by subjects.

$$SFI = s \times \alpha = \frac{\sqrt{\frac{1}{N}\sum_{i=1}^{N}(y(i)-\bar{y})^2}}{\bar{y}} \times \frac{\sum_{i=1}^{N}\theta_i}{T} \quad (°/min) \tag{7}$$

2.3.2 Mixed Perception Index

To observe the "mixed" dynamic perceptual mode and utilize it to represent the actual overall thermal comfort, the thermal sensation and thermal pleasure answered during experiments were integrated into a mixed perception index (*MP*). As shown in Eq. (9), *MP* is defined as the ratio of normalized transient thermal sensation vote (*nTSVt*) to transient thermal pleasure (*TPt*) *nTSVt* values ranging from 0 to 1 are determined using Eq. (8), where $TSVt_{min}$ corresponds to "-3" and $TSVt_{max}$ refers to "3", expressing thermal sensation from cold (-3) to hot (3). As a result, the range of *MP* is from 0 to 1, and the smaller the *MP* value, the more inclined to comfort.

$$nTSVt = \frac{TSVt - TSVt_{min}}{TSVt_{max} - TSVt_{min}} \tag{8}$$

$$MP = \frac{nTSVt}{TPt} = \frac{TSVt+3}{6TPt} \tag{9}$$

2.3.3 Overall Need Index

To identify if stronger variations in wind and solar radiation have favorable influences on pedestrians' thermal comfort, the overall need for lowering air temperature in a walking period requires observations. As a result, equation (10) is intended to describe the overall need for

lowering air temperature based on the responses to question 3.The greater the $\text{Need}_{lower\_T_a}$ value, the greater the need to reduce the overall air temperature during walking.

$$\text{Need}_{lower\_T_a} = \frac{\sum_1^n Scale_{Ta}}{15n} \quad (n > 1) \qquad (10)$$

where, $Scale_{Ta}$ presents the need level for lowering T_a in one answer; n presents the total number of answers to question 3 in a walking period; "*15*" means the maximum need level for changing T_{mrt}, v, and T_a in one answer. The overall need for lowering air temperature is denoted as N_{L_Ta}.

3. Results and Discussions

3.1 Meteorological parameters and their variations

Figure 7 shows the samples of T_a, T_g, and v collected thoughout the walking period on various experimental days. The legend in Figure 7 depicts the average air temperature during the walking period on one experimental day, and the abscissas show the walking period. As introduced in Section 2.3.1, the variation of a parameter was described by the coefficient of variation (*cv*) in a mathematical perspective and the rotation angle (θ_i) in a geometrical perspective. As seen from Figure 7, the variations of T_g and v are much more intense and visible than those of air temperature during the experiments. Moreover, they are distinctive on different experimental days, demonstrating a considerable variation in wind and solar radiation when walking in urban continuums and emphasizing the importance of categorizing these variations to assess their impacts on thermal comfort.
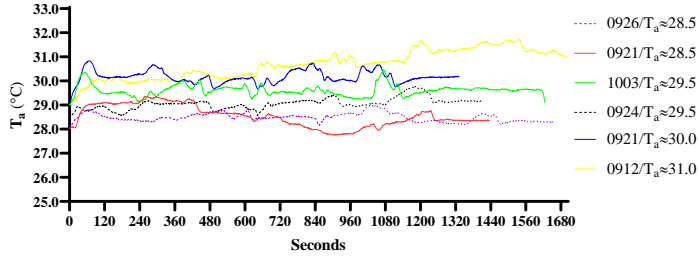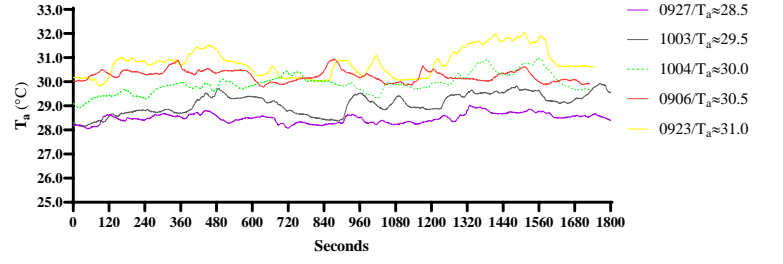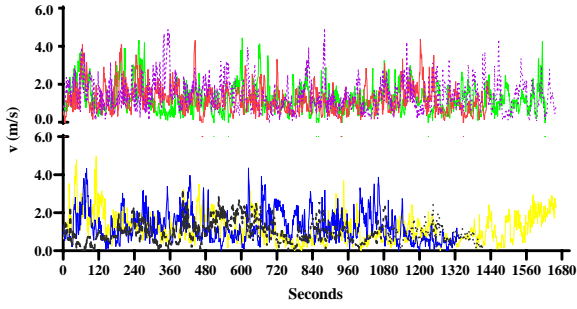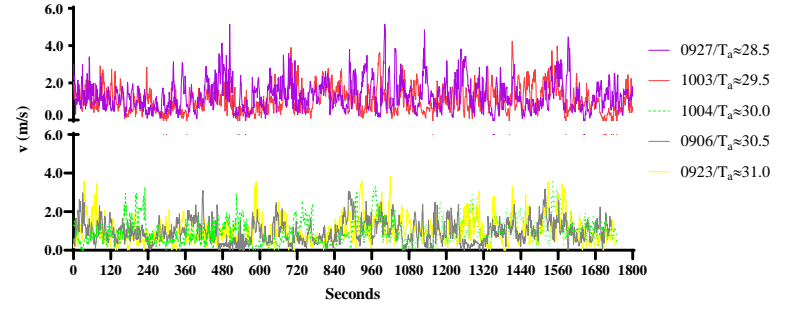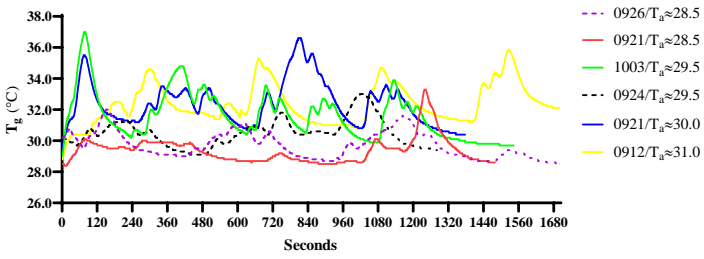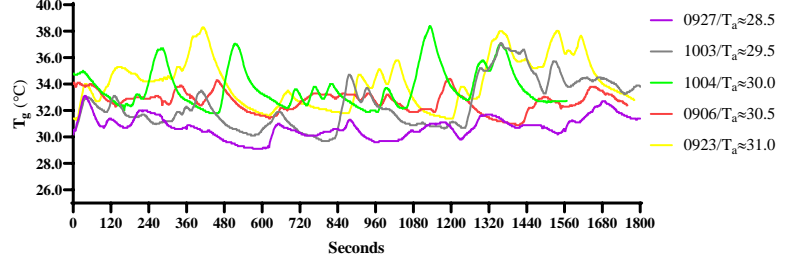
Figure 6. The measured T_a, v and T_g in walking period on several experimental days: a) measured T_a on campus; b) measured T_a in urban streets; c) measured v on campus; b) measured v in urban streets; e) measured T_g on campus; f) measured T_g in urban streets.

In order to quantify these variations and analyze their impacts, this study focuses on the variation in wind and solar radiation that can be sensed by subjects during walking, which is

19

supposed to play a central role in thermal comfort. In view of this, meteorological parameters corresponding to transient question answers during walking periods were extracted. Given the proposed Sensed Variation Index (*SVI*) in Section 2.3.1, the variation of v (SVI_v) and that of T_{mrt} (SVI_{mrt}) were calculated for each walking period using Eqs. (3-7).

Figure 7 firstly displays the distributions of meteorological parameters corresponding to transient answers. Based on the percentage of a meteorological parameter's values rounded to bin centers, T_{mrt} on campus concentrates on the smaller side and v on campus concentrates on the larger side. During walking states, T_{mrt}, v, T_a and RH range from 28.0 ℃ to 60.0℃, 0 m/s to 5.5 m/s, 28.0 ℃ to 33.0℃, and 60% to 80%, respectively. Illustrated from Table 1, the prevailing wind directions measured by Hong Kong King's Park Weather Station near the experiment sites are from 90° to 110° (east wind) during experiments.
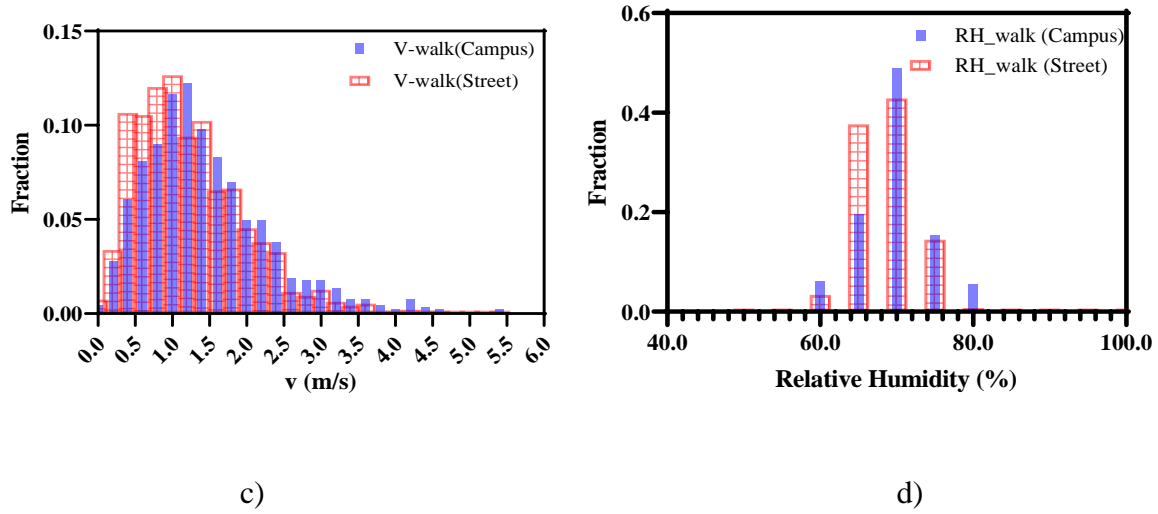

a)   b)

c)

d)
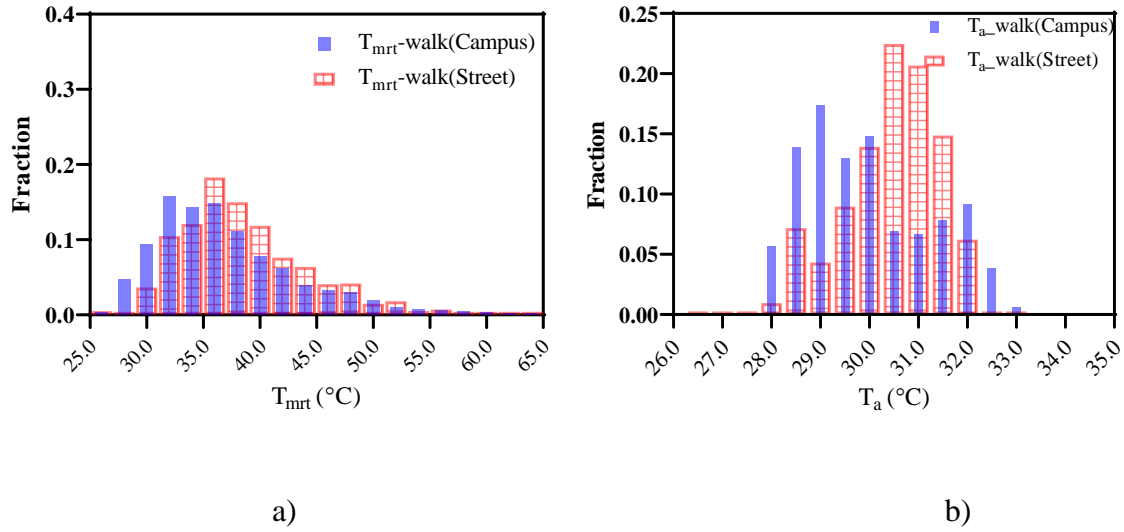
Figure 7 Measured meteorological parameters corresponding to each questionnaire survey during walking periods: a) mean radiant temperature T_{mrt}; b) air temperature T_a; c) wind speed v; d) relative humidity RH.
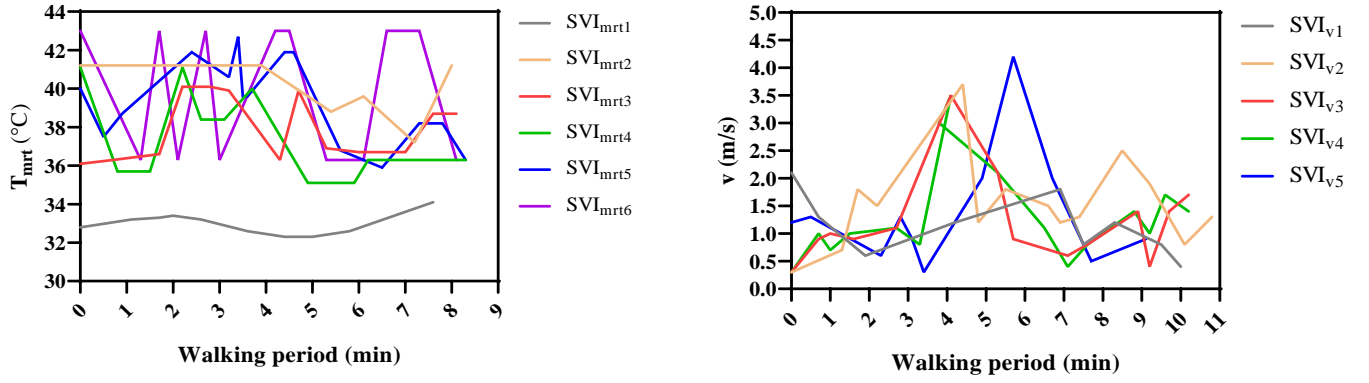
The histogram distribution of SVI_{mrt} and SVI_v values is displayed in Figure 8a, and the larger value indicates the more intense variation that was sensed by subjects. The abscissa in Figure 8a shows the bin center of an SFI_{mrt} bin with a 1°/min width and the bin center of an SFI_v bin with a 10°/min width. From Figure 8a, SVI_{mrt} is larger than 0 but lower than 22°/min, generally smaller than that of SVI_v, which is larger than 0 but smaller than or equal to 100°/min, indicating a more intense wind variation sensed by pedestrians. Based on the number of values located in each SVI_{mrt} bin, SVI_{mrt} values are divided into 6 ranges to classify the variation level of T_{mrt}: level 1 with 0≤ SVI_{mrt}≤0.5°/min; level 2 with 0.5< SVI_{mrt}≤1.5°/min; level 3 with 1.5< SVI_{mrt}≤2.5°/min; level 4 with 2.5< SVI_{mrt}≤4.5°/min; level 5 with 4.5< SVI_{mrt}≤6.5°/min; level 7 with SVI_{mrt}>6.5°/min. Similarly, the SVI_v values are divided into 5 ranges: level 1 with SVI_v≤15°/min; level 2

with $15 < SVI_v \leq 25°/min$; level 3 with $25 < SVI_v \leq 35°/min$; level 4 with $35 < SVI_v \leq 45°/min$; level 5 with $SVI_v > 45°/min$.

Given the classification of SVI_{mrt} and SVI_v values, Figure 8b gives an example of extracted T_{mrt} and v against time under different SVI_{mrt} and SVI_v levels. The variations of wind and solar radiation that are supposed to play a central role in thermal comfort were thus extracted. From the Figure, the variation shapes of T_{mrt} and v, which are reflected by coefficient of variation and rotation angle, are unique under different variation levels, demonstrating that the SVI si suitable to characterize influential variations in T_{mrt} and v.
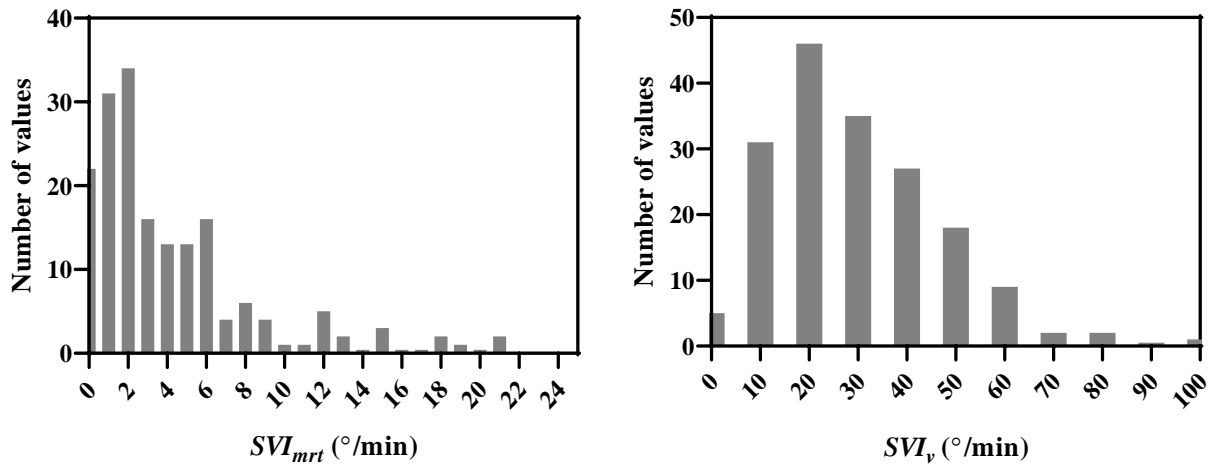

a)

b)

Figure 8 SVI_{mrt} and SVI_v classification: a) histogram distribution of SVI_{mrt} and SVI_v; b) variation samples of T_{mrt} and v corresponding to transient TSV at various fluctuation levels.
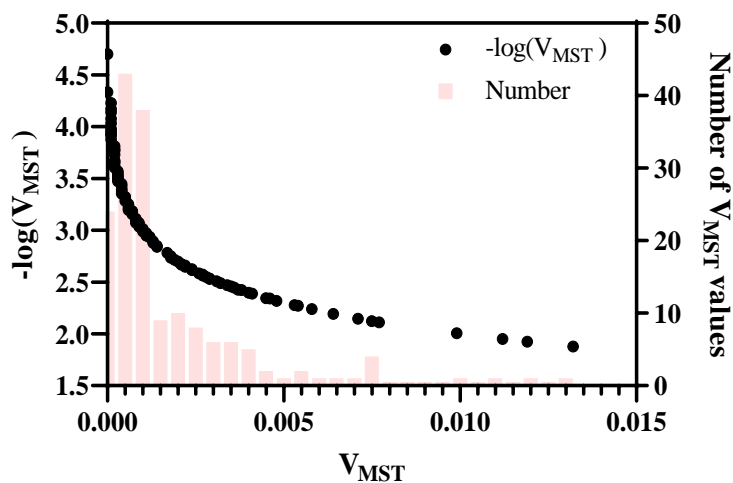
3.2 Skin temperature and its variation

Skin temperature measured in the walking period is observed in this section. Due to the possible delay of skin temperature change responding to the changes in v and T_{mrt}, the local skin temperature after one change in v or T_{mrt}, in other words, after one transient TSV, is determined by the average value of local skin temperatures measured in the interval between this transient TSV and the next transient TSV. The determination is based on the assumption that there is no significant environmental change in this interval, so the skin temperature won't be influenced significantly by other factors and only gradually show the change induced by the prior environmental change. Consequently, the mean skin temperature responding to the transient TSV was calculated using these temperatures.

Figure 9a shows the distribution of female and male subjects' local skin temperatures and mean skin temperatures (MST) corresponding to changes in v or T_{mrt}, in other words, transient TSVs. The box and whiskers reflect the interquartile range and the 1.5 times interquartile range,

23

respectively, and the 1.5 times interquartile range is used to detect the outliers. As seen from Figure 9a, the comparable skin temperatures of the head parts (cheek, forehead, and neck) and core parts (chest, back, and abdomen) found in this study were resulted from wearing a mask and direct sunlight on the head during experiments. The mean skin temperature range for female subjects is from 32.04 °C to 35.76 °C, whereas that for male subjects is from 32.43 °C to 35.63 °C. The results of skin temperature are reliable because of the comparable range of skin temperatures seen on campus and in the street under similar thermal conditions.
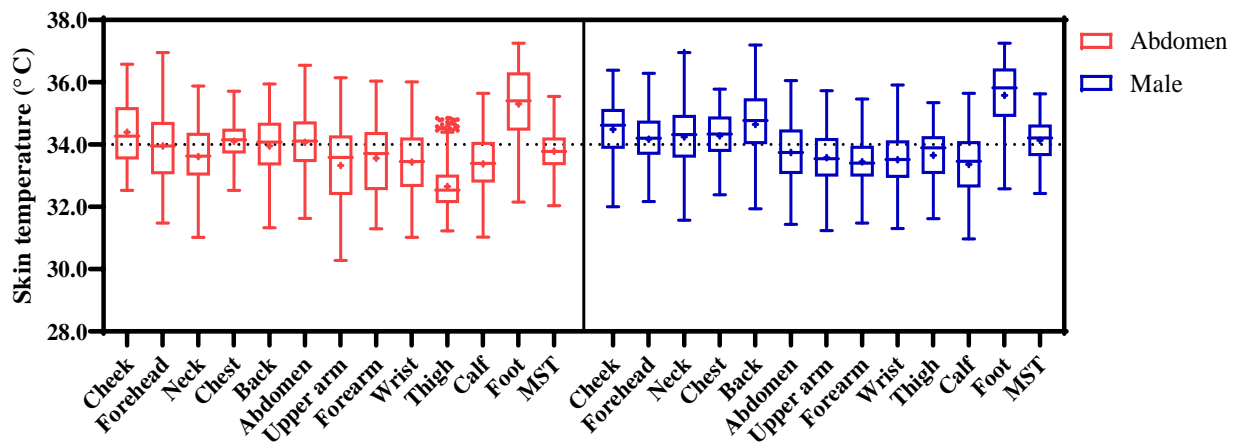
a)

b)
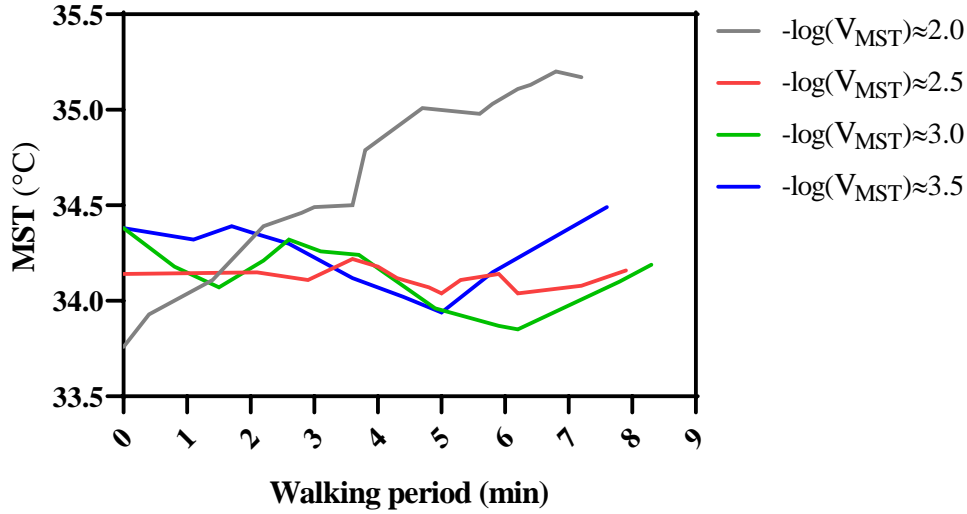
c)

Figure 9 Skin temperature and its variation during walking period: a) distributions of local skin temperature and mean skin temperature of female and male subjects; b) mean skin temperature variability (V_{mst}); c) examples of *MST* variation corresponding to -log (V_{mst}) bin center.

As introduced above, the feature of simultaneous variations in wind and solar radiation is expected to be equivalent to the variability of skin temperature; therefore, the *MST* variability (V_{MST}) was determined using the same method of calculating variations in solar radiation and wind. Due to small calculated V_{MST} values, however, V_{MST} values were transferred to *-log (V_{MST})* values of greater than 1, and the smaller the -log(V_{MST}) value, the greater the *MST* variability. Figure 9b shows the conversion of V_{MST} to *-log (V_{MST})* and the histogram distribution, indicating a range of *-log (V_{MST})* from 2.0 to 4.5. Figure 9c displays the examples of variation in *MST* grouped by different -log (V_{MST}) bin centers, verifying different variations of *MST* through the coefficient of variance and rotation angle.

3.3 Impacts of simultaneous SVI_v and SVI_{mrt}

3.3.1 Impacts of simultaneous SVI_v and SVI_{mrt} on mixed thermal perceptions

Figure 10 shows the variation of transient mixed perception (MPt) rounded to 0.1 against $TSVt$ under different TPt values, revealing the mixed thermal perceptions during experiments. It can be seen that "$MPt \approx 0.1$" corresponds to $TSVt$ of around -1 (slightly cool) and pleasure feeling ("$TPt=3$"); "$MPt \approx 0.2$" corresponds to $TSVt$ from -1.5 (slightly cool) to 1.5 (slightly warm) and okay or pleasure feeling ("$TPt=2$ or 3"); "$MPt \approx 0.3$" corresponds to $TSVt$ from 0 (neutral) to 3 (hot) and okay or pleasure feeling ("$TPt=2$ or 3"); "$MPt \approx 0.4$" and "$MPt \approx 0.5$" correspond to $TSVt$ from 1 (slightly warm) to 3 (hot) and okay feeling ("$TPt= 2$"); "$MPt>0.5$" corresponds to $TSVt$ over 0 (neutral) and annoyed feeling ("$TPt=1$"). MPt values ranging from 0.1 to 0.3 indicate comfort-biased thermal states, 0.4 to 0.5 indicate warm-but-normal thermal states, and greater than 0.5 indicate discomfort-biased thermal states. In view of this, MPt is assumed to be a continuous variable, and the smaller the MPt value, the more comfortable mixed thermal perceptions it indicates.
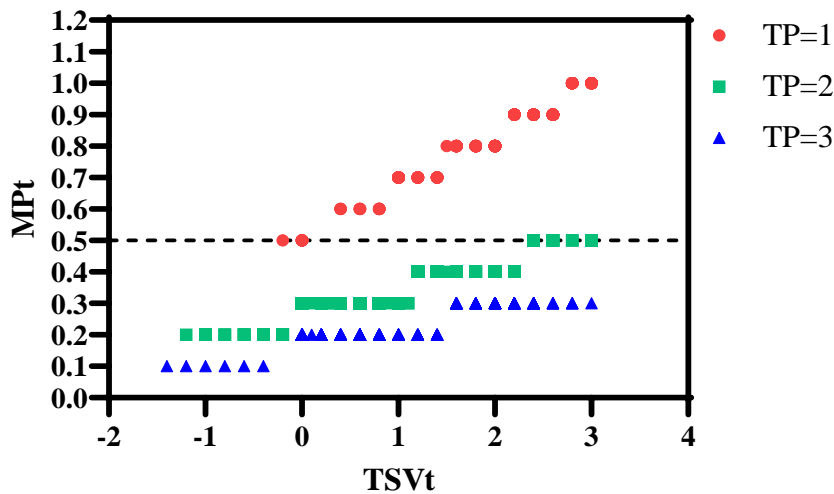
Figure 10 Distribution of *MPt* against *TSVt* regarding to different *TP* values.

Given the *MPt*, impacts of SVI_v on *MPt* were investigated by the Pearson correlation analysis between SVI_v and *MPt* under each SVI_{mrt} level and two air temperature ranges, and the results are shown in Table 5.

Table 5 The Pearson correlation analysis between SVI_v and *MPt* for each SVI_{mrt} level

SVI_v vs. *MPt*	T_a range	SVI_{mrt1}	SVI_{mrt2}	SVI_{mrt3}	SVI_{mrt4}	SVI_{mrt5}	SVI_{mrt6}
Pearson coefficient		-0.3145	-0.3029	-0.3776	-0.3494	-0.4321	-0.3429
95% confidence interval	$T_a < 30.0°C$	-0.5104 to -0.08767	-0.4573 to -0.1307	-0.5406 to -0.1873	-0.4818 to -0.2014	-0.5807 to -0.2556	-0.6259 to 0.01981
P value (two-tailed)		0.0076	0.0008	0.0002	<0.0001	<0.0001	0.0636
Significant? (alpha = 0.05)		Yes	Yes	Yes	Yes	Yes	No
Number of XY Pairs		71	120	92	152	98	30
Pearson r		0.05877	-0.08809	-0.1601	-0.4146	0.04719	-0.04621
95% confidence interval		-0.2323 to 0.3402	-0.2734 to 0.1035	-0.2880 to -0.02654	-0.5694 to -0.2314	-0.09215 to 0.1847	-0.1691 to 0.07806
P value (two-tailed)	$T_a \geq 30.0°C$	0.6948	0.3669	0.0191	<0.0001	0.5069	0.4661
Significant? (alpha = 0.05)		No	No	Yes	Yes	No	No
Number of XY Pairs		47	107	214	94	200	251

As seen from Table 5, when the T_a was lower than 30.0 °C, despite the relatively small value of the Pearson coefficient, *MPt* is verified to decrease with increasing SVI_v under a SVI_{mrt} level. Therefore, the more intense wind variation during walking, the more the subjects were inclined to comfort. However, when the T_a is larger than 30.0 °C, the Pearson coefficient reduces and the significant correlation is only found under SVI_{mrt3} and SVI_{mrt4}. The results demonstrate that higher temperatures can mitigate the impacts of SVI_v on *MPt*.

Similarly, the impacts of SVI_{mrt} on MPt were investigated by the Pearson correlation analysis between SVI_{mrt} and MPt for each SVI_v level and for two air temperature ranges. The results are shown in Table 6. A positive correlation between SVI_{mrt} and MPt was observed when the T_a was lower than 30.0 °C, meaning that MPt increased SVI_{mrt} as rose. The results demonstrate that the more intense the T_{mrt} variation subjects experienced, subjects were more likely to feel uncomfortable. This correlation, however, was only found significant when the SVI_v level is between 2 and 4, which may be due to less effective variations in solar radiation on MPt if there is a very strong or weak variation in wind. The Pearson coefficients declined much further when the T_a exceed 30.0°C, as shown in Table 5.

Table 6 The Spearman correlation analysis between SFI_{mrt} and MPt for each SFI_v level under T_a<30.0°C

SVI_{mrt} vs. MPt	T_a range	SVI_{v1}	SVI_{v2}	SVI_{v3}	SVI_{v4}	SVI_{v5}
Pearson r		0.1712	0.3830	0.3309	0.3513	0.1354
95% confidence interval		-0.0115 to 0.3428	0.2378 to 0.5114	0.1329 to 0.5035	0.1693 to 0.5102	-0.0597 to 0.3205
P value (two-tailed)	T_a<30.0°C	0.0662	<0.0001	0.0014	0.0003	0.1726
Significant? (alpha = 0.05)		No	Yes	Yes	Yes	No
Number of XY Pairs		116	151	90	103	103
Pearson r		0.03342	0.1245	0.2096	0.1467	0.1564
95% confidence interval		-0.1583 to 0.2228	-0.0104 to 0.2550	0.0796 to 0.3327	-0.0203 to 0.3057	0.0265 to 0.2812
P value (two-tailed)	T_a≥30.0°C	0.7338	0.0705	0.0018	0.0849	0.0186
Significant? (alpha = 0.05)		No	No	Yes	No	Yes
Number of XY Pairs		106	212	220	139	226

Illustrated from Table 5 and Table 6, there are cooling effects of stronger variation in wind, which agrees with the results found by Yu et al. (2020), who observed that increasing wind

turbulence intensity will increase convective heat transfer and bring about cooling effects during wind tunnel testing. In the real scenario, however, such cooling effects should be simultaneously affected by air temperature and variations in solar radiation. Additionally, an increase in air temperature will reduce the impacts of wind and solar radiation variations on mixed perceptions.

3.3.2 Impacts of simultaneous SVI_v and SVI_{mrt} on -log(V_{MST})

Due to the finding in Section 3.3.1 that the effects of variations in wind and solar radiation on MPt are complicated, the integrated impacts of SVI_v, SVI_{mrt} and air temperature on -log(V_{MST}) were analyzed using the multiple linear regression for each subject during each walking period. The regression analysis results are reported in Table 7.

Table 7 Multiple linear regression analysis results

Model Abstract			
	R squared	0.541	
Goodness of fit	Significance	0.000	
	F	42.317	
Input variable			
	SVI_{mrt}	SVI_v	T_a
Coefficient	-0.043	-0.013	-0.091
Normalized coefficient	-0.328	-0.421	-0.193
Significance	0.000	0.000	0.002

According to Table 7, R^2 of the multiple line model is 0.541, indicating that input variables SVI_v, SVI_{mrt} and T_a can explain around 54% of the -log(V_{MST}) values in this study. In this model, the coefficients of SVI_v, SVI_{mrt} and T_a are negative and significant, validating that MST variability

is caused by the variations in wind and solar radiation and that V_{MST} increases as SVI_v, SVI_{mrt} and T_a increase. Meanwhile, an increase in V_{MST} indicates an intensified heat exchange between the human body and its surroundings. The normalized coefficients in Table 7 explain that the contribution of SVI_v on $-\log(V_{MST})$ is greater than that of SVI_{mrt} and T_a. Notably, the impacts of T_a on $-\log(V_{MST})$ are attributed to the fact that T_a affects the magnitude of MST, which is used to determine $-\log(V_{MST})$.

The R^2 of 0.54 in Table 7 might be attributed to the delay of measured skin temperature in responses to the changes in wind speed and solar radiation, despite the fact that the averaged skin temperature in the interval between two environmental changes was calculated to offset the delay effect. On the other hand, a complex nonlinear relationship may occur between variations in wind, solar radiation, and MST variability, as opposed to a linear relationship. Nevertheless, the simultaneous variations in wind and solar radiation can be characterized by the MST variability using Equation (11), identifying the intensity or level of dynamic thermal environments with varying wind and solar radiation and making it possible to estimate thermal comfort in complex environments.

$$Predicted\ (-\log(V_{MST}))\ or\ R\_DTE = 6.356 - 0.043 \times PVI_{mrt} - 0.013 \times PVI_v - 0.091 \times T_a$$

(11)

The left-hand side of Eq. (11) depicts the predicted MST variability or the reverse dynamic thermal environment (R_DTE), which is characterized by rapidly varied wind and solar radiation.

3.4 Evaluation of thermal comfort with R_DTE

3.4.1 Need for lowering air temperature against R_DTE

To explore if simultaneously varying wind and solar radiation have positive effects on thermal comfort during walking, the need for lowering air temperature (N_{L_Ta}) was determined for each walking period using Eq. (10) in Section 2 and then averaged under each R_DTE bin center on campus and in the street, as shown in Figure 11. The linear regression analysis was conducted for N_{L_Ta} and R_DTE, and is displayed in Figure 11.
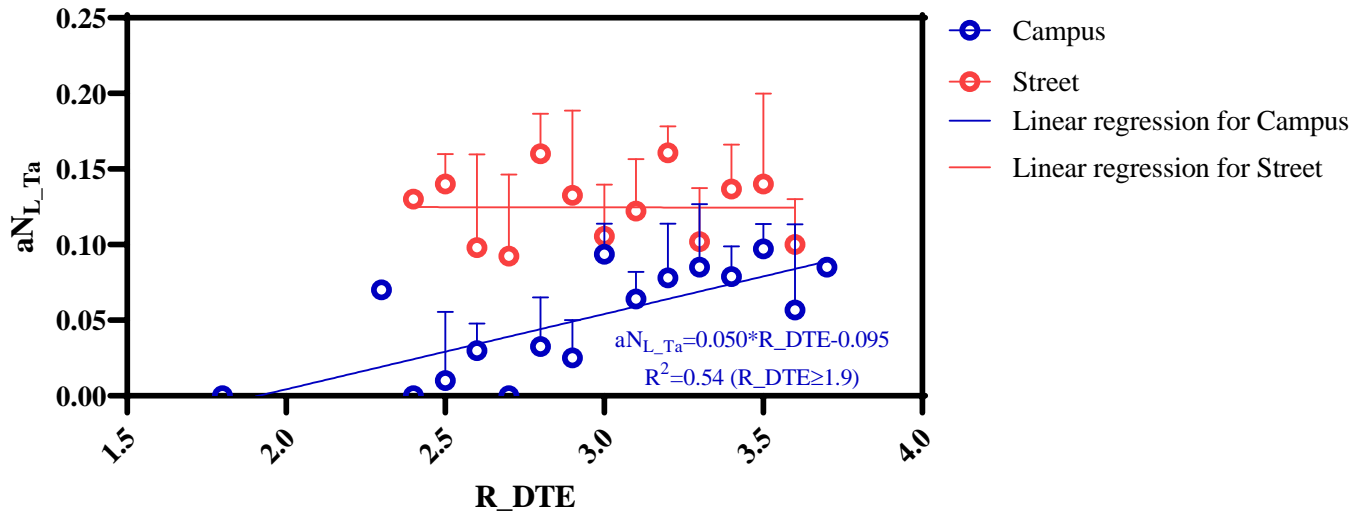

Figure 11 The average need for lowering air temperature (N_{L_Ta}) against R_DTE values rounded to 0.1-bin.

Figure 11 shows the variation of the average cooling demand (aN_{L_Ta}) versus R_DTE in the street and on campus. It can be seen that the variation of aN_{L_Ta} on campus is positively linear with respect to R_DTE, suggesting that the need for lowering air temperature reduces as the intensity of varied wind and solar radiation (dynamic environment) increases. It is expected that stronger dynamic thermal environments will reduce the effects of high air temperature. The

phenomenon might be attributed to faster heat transfer over the skin surface, which renders subjects less sensitive to ambient temperature. If R_DTE decreases from 3.7 to 1.9 on campus, the aN_{L_Ta} value will decrease by about 0.1, and the overall need scales for lowering air temperature will reduce by 0.1 times 15n scales in a walking period (seeing Eq. 10). For example, if three thermal needs interviews (n=3) are conducted during a walking period, the total need scales of reducing air temperature will fall by 4 to 5 scales.

However, the aN_{L_Ta} in the street is not only greater than that on campus, but also does not significantly change with R_DTE. The outcomes may have been influenced by different street and campus characteristics. In this study, the street was more populated and closer to vehicles than the campus, and the people and vehicles acted as heat sources and CO_2 sources, which boosted greenhouse effects and the radiant heat transfer from the ambient settings to the human body. These radiations may not be easily and completely detected by the globe temperature sensors, but they make people feel hotter and increase the desire to reduce air temperature. Under such conditions, variations in wind and solar radiation exert little influences on the thermal conditions of people.
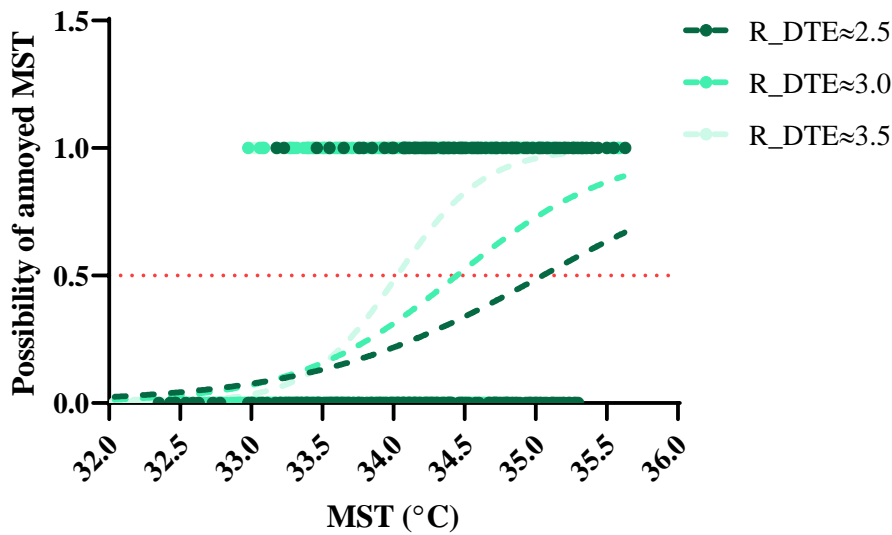
3.4.2 Pleasant air temperature and pleasant mean skin temperature

Given the result in Figure 11 that dynamic thermal environments with simultaneously varying wind and solar radiation can influence the acceptance of air temperature, a temperature range corresponding to the N_{L_Ta} bin with 0.1 width was thus observed under each R_DTE bin with 0.5 width (Figure 12). The abscissa of Figure 12 shows R_DTE values, and the lower the value, the stronger the dynamic thermal environments are. In the N_{L_Ta} bin with the center of 0.1, there is less need for lowering air temperature; hence, the corresponding average air temperature is regarded as the pleasant air temperature and found to decrease as R_DTE increases. The findings

indicate that as the dynamic environments become stronger, from *R_DTE* of 3.5 to *R_DTE* of 2.5, the pleasant average air temperature rises by about 2.0 °C, from 29.0 °C to 31.0 °C. Similar results are observed for N_{L_Ta} bin with a center of 0.2. In general, enhancing the intensity of dynamic thermal environments characterized by varied wind and solar radiation is believed to mitigate the impacts of high air temperatures (lower than 34.0°C) on hot summer days.
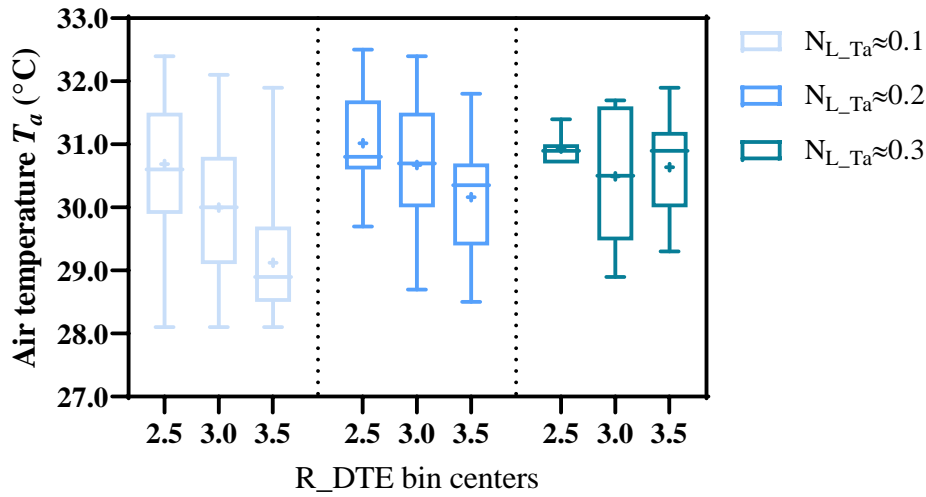
a)

b)

Figure 12 Impacts of *R_DTE* on a) pleasant air temperature and b) threshold of annoyed mean skin temperature

Under *R_DTE,* in addition to pleasant air temperature, a mean skin temperature that elicits pleasant or annoyed feelings was observed. To explore the threshold of *MST_annoyed*, under each *R_DTE* bin with 0.5 width, *MST* corresponding to transient mixed perception "*MPt*≤0.4" was assumed to have a 0% probability of triggering annoyed feelings. Meanwhile, *MST* corresponding to "*MPt*>0.4" was judged to have a 100% probability of triggering annoyed feelings. Based on the probability distributions of annoyed *MST* ($MST_{MPt>0.3}$) and pleasant *MST* ($MST_{MP\leq0.3}$), a simple logistic regression model was proposed to predict the threshold of annoyed *MST*; the results are shown in Figure 13 and Table 8. The Tjur's R squared and area under the ROC curve in Table 8 examine the reliability of simple logistic regression results, and the likelihood ratio test with a P value lower than 0.05 confirms that the slope of the simple logistic model is significantly different from 0 (Motulsky, 2016; Steenackers et al., 1989).

Table 8 Simple logistic models for the probability of annoyed *MST*

R_DTE bin center	*MST_annoyed* Threshold (*MST* at 50%)	Tjur's R squared	Area under the ROC curve	Likelihood ratio test (P value)	Proportion of "*MPt*>0.4" under *MST*≥*MST_annoyed*
0.25	35.2	0.1537	0.7017	<0.0001	72.8%
0.30	34.5	0.2104	0.7652	<0.0001	79.9%
0.35	34.0	0.4314	0.8942	<0.0001	91.1%

In Figure 12, the X values of crossings for the "Y=0.5" line and three regression curves are thresholds of *MST_annoyed* under different levels of dynamic thermal environments, which means that *MST* exceeding the threshold of *MST_annoyed* under one level of dynamic environment has a high likelihood of making people annoyed. Figure 12 reveals that the *MST_annoyed* thresholds for *R_DTE* bin centers of 2.5, 3.0, and 3.5 are 35.2 ℃, 34.5 ℃, and 34.0 ℃, respectively, indicating the stronger the dynamic thermal environments, the higher the *MST_annoyed* threshold. Due to the different intensities of dynamic thermal environments with varied wind and solar radiation, the largest difference in *MST_annoyed* threshold reaches 1.2℃. The results could be attributed to the delayed subjects' perceptions in response to rapid changes in mean skin temperature, which is opposed to the "alliesthesia" effects. Nevertheless, it seems that as long as the *MST* is larger than 35.2 ℃, it has the great possibility of irritating people, regardless of stronger dynamic thermal environments. To verify the accuracy of the predicted threshold *MST_annoyed*, the probability of "*MPt*>0.4" was examined under *MST* greater than *MST_annoyed*. As seen from Table 8, these probabilities are all greater than 50.0%, demonstrating the correct *MST_annoyed* threshold.

5. Conclusion

This study overcomes the challenge of evaluating the influences of thermal environments with rapid and simultaneous variations in wind and solar radiation on "mixed" thermal perceptions and verifies the favorable effects of strengthening both variations in wind and solar radiation on the acceptance of high air temperature. The main conclusions were obtained as follows:

There are different intensities of variations in wind and solar radiation that can be sensed during walking in the urban continuum, and mixed thermal perception (*MP*) will occur when these variations are encountered. *MP* values between 0.1 and 0.3 suggest comfort-biased thermal

states, those between 0.4 and 0.5 refer to warm-but-normal thermal states, and those greater than 0.5 refer to discomfort-biased thermal states. *MP* will reduce as the intensity of variations in wind increases, but this relationship is weakened by a higher temperature. *MP* will increase as the intensity of variation in solar radiation increases, but this relationship is also affected by how the wind and air temperature change.

On summer days, subjects' mean skin temperature (MST) range from 32.04 ℃ to 35.76 ℃ while walking in the street and on campus. MST will also vary at different levels, and this variability is determined by the air temperature and the variations in wind and solar radiation in a multiple linear model, in which the contribution of variations in wind is larger than that of variations in solar radiation. The model called R_DTE can be used to characterize the intensity of dynamic thermal environments characterized by simultaneous variations in wind and solar radiation. The larger the skin temperature variability, the more intense such dynamic thermal environment are.

When the air temperature is below 34.0 ℃, an increase in the intensity of simultaneously varying wind and solar radiation, or an increase in the MST variability, reduces the need for lowering the air temperature, and a two-degree increase in the air temperature acceptability is possible. However, this phenomenon is not obvious in the crowded and noisy urban streets. Additionally, a rise in the intensity of variations in wind and solar radiation can increase the threshold of MST that irritates people, which may be related to the delayed perceptions of rapid changes in skin temperature rather than "alliesthesia" effects. However, as long as the MST is over 35.2 ℃, it has a high potential to irritate people, regardless of stronger variations in wind and solar radiation.

This study thus proposes a method to characterize the level of dynamic thermal environments characterized by varied wind and solar radiation using the MST variability for estimating thermal comfort during walking and to inspire urban designers to take advantage of varying wind and solar radiation in the urban continuums to improve pedestrians' thermal experience in warm-to-hot climate regions. The work is anticipated to inform the further study on the dynamic thermal comfort and optimal combination of varied wind and solar radiation for thermal comfort while walking. Due to the length limit of the article, the convective, radiative, and evaporative heat exchange in response to variations in wind and solar radiation will be discussed in the following article.

Acknowledgements

6. Reference

Ahmed-Ouameur, F., & Potvin, A. (2007). *Microclimates and thermal comfort in outdoor pedestrian spaces a dynamic approach assessing thermal transients and adaptability of the users.* Paper presented at the Proceedings of the solar conference.

ASHRAE. (2013a). ANSI/ASHRAE Standard 55-2013, Thermal Environmental Conditions for Human Occupancy. *Atlanta: ASHRAE.*

ASHRAE. (2017). Chapter 9, ASHRAE Handbook—Fundamentals. *Atlanta: ASHRAE.*

Asimakopoulos, D., Santamouris, M., Farrou, I., et al. (2012). Modelling the energy demand projection of the building sector in Greece in the 21st century. *Energy and Buildings, 49*, 488-498.

Cao, S., Ming, P, & Zhao, X. (2021). Fuzzy comprehensive evaluation of human thermal comfort in simulating natural wind environment. *Building and Environment, 188*, 107447.

de Dear, R. (2011). Revisiting an old hypothesis of human thermal perception: alliesthesia. *Building Research & Information, 39*(2), 108-117. doi:10.1080/09613218.2011.552269

De Dear, R., Ring, J., & Fanger, P. (1993). Thermal sensations resulting from sudden ambient temperature changes. *Indoor air, 3*(3), 181-192.

Fiala, D. (1998). *Dynamic simulation of human heat transfer and thermal comfort.* De Montfort University Leicester, UK,

Fiala, D., & Lomas, K. (2001). *The dynamic effect of adaptive human responses in the sensation of thermal comfort.* Paper presented at the Proceedings Windsor Conference.

Frank, S. M., Raja, S. N., Bulcao, C. F., & Goldstein, D. S. (1999). Relative contribution of core and cutaneous temperatures to thermal comfort and autonomic responses in humans. *Journal of applied physiology, 86*(5), 1588-1593.

Guan, Y. D., Hosni, M. H., Jones, B. W., & Gielda, T. P. (2003). Investigation of human thermal comfort under highly transient conditions for automotive applications-part 2: Thermal sensation modeling. *Ashrae Transactions, 109*, 898.

HKO. (2020). Monthly Extract of Meteorological Observations, 2020 (Publication no. https://www.hko.gov.hk/en/cis/monthlyExtract.htm?y=2020). from Hong Kong Obervatory

Hodder, S. G., & Parsons, K. (2007). The effects of solar radiation on thermal comfort. *International Journal of Biometeorology, 51*(3), 233-250.

Houdas, Y., & Ring, E. F. J. (1982). *Human Body Temperature: Its Measurement and Regulation*.

Huang, L., Ouyang, Q., & Zhu, Y. (2012). Perceptible airflow fluctuation frequency and human thermal response. *Building and Environment, 54*, 14-19.

ISO. (2005). Analytical Determination and Interpretation of Thermal Comfort using Calculation of the PMV and PPD Indices and Local Thermal Comfort Criteria. *Standard 7730-2005, Ergonomics of the thermal Environment*.

Kingma, B. R., Vosselman, M., Frijns, A., Van Steenhoven, A., & van Marken Lichtenbelt, W. (2014). Incorporating neurophysiological concepts in mathematical thermoregulation models. *International Journal of Biometeorology, 58*(1), 87-99.

Lai, D., Lian, Z., Liu, W., et al. (2020). A comprehensive review of thermal comfort studies in urban open spaces. *The Science of the total environment, 742*, 140092-140092. doi:10.1016/j.scitotenv.2020.140092

Lai, D., Zhou, X., & Chen, Q. (2017). Measurements and predictions of the skin temperature of human subjects on outdoor environment. *Energy and Buildings, 151*, 476-486.

Li, J., Niu, J., Huang, T., & Mak, C. M. (2022). Dynamic effects of frequent step changes in outdoor microclimate environments on thermal sensation and dissatisfaction of pedestrian during summer. *Sustainable Cities and Society*, 103670.

Li, J., Niu, J., Mak, C. M., Huang, T., & Xie, Y. (2020). Exploration of applicability of UTCI and thermally comfortable sun and wind conditions outdoors in a subtropical city of Hong Kong. *Sustainable Cities and Society, 52*, 101793.

Liu, S., Nazarian, N., Hart, M. A., Niu, J., Xie, Y., & de Dear, R. (2021). Dynamic thermal pleasure in outdoor environments - temporal alliesthesia. *Sci Total Environ, 771*, 144910-144910. doi:10.1016/j.scitotenv.2020.144910

Liu, W., Lian, Z., Deng, Q., & Liu, Y. (2011). Evaluation of calculation methods of mean skin temperature for use in thermal comfort study. *Building and Environment, 46*(2), 478-488. doi:10.1016/j.buildenv.2010.08.011

Ouyang, Q., Dai, W., Li, H., & Zhu, Y. (2006). Study on dynamic characteristics of natural and mechanical wind in built environment using spectral analysis. *Building and Environment, 41*(4), 418-426.

Parkinson, T., de Dear, R., & Candido, C. (2016). Thermal pleasure in built environments: alliesthesia in different thermoregulatory zones. *Building Research & Information, 44*(1), 20-33.

Shimazaki, Y., Yoshida, A., Suzuki, R., Kawabata, T., Imai, D., & Kinoshita, S. (2011). Application of human thermal load into unsteady condition for improvement of outdoor thermal comfort. *Building and Environment, 46*(8), 1716-1724.

Takada, S., Kobayashi, H., & Matsushita, T. (2009). Thermal model of human body fitted with individual characteristics of body temperature regulation. *Building and Environment, 44*(3), 463-470.

Vasilikou, C., & Nikolopoulou, M. (2020). Outdoor thermal comfort for pedestrians in movement: thermal walks in complex urban morphology. *International Journal of Biometeorology, 64*(2), 277-291.

Wang, X., Mei, Y., Cai, H., & Cong, X. (2016). A new fluctuation index: characteristics and application to hydro-wind systems. *Energies, 9*(2), 114.

WHO. (2018). Heat and Health. Retrieved from https://www.who.int/news-room/fact-sheets/detail/climate-change-heat-and-health

WMO. (2022). Heat, drought and wildfires during one of the warmest Julys on record. Retrieved from https://news.un.org/en/story/2022/08/1124242

Xia, Y., Nm, J., & BURNETT, J. (2000). Effects of Turbulent Air on Human Thermal Sensations in a Wann Isothermal Environment. *Indoor air, 10*, 289-296.

Xie, Y., Huang, T., Li, J., et al. (2018). Evaluation of a multi-nodal thermal regulation model for assessment of outdoor thermal comfort: Sensitivity to wind speed and solar radiation. *Building and Environment, 132*, 45-56.

Yang, W., Wong, N. H., & Jusuf, S. K. (2013). Thermal comfort in outdoor urban spaces in Singapore. *Building and Environment, 59*, 426-435.

Yu, Y., de Dear, R., Chauhan, K., & Niu, J. (2021). Impact of wind turbulence on thermal perception in the urban microclimate. *Journal of Wind Engineering and Industrial Aerodynamics, 216*, 104714.

Yu, Y., Liu, J., Chauhan, K., de Dear, R., & Niu, J. (2020). Experimental study on convective heat transfer coefficients for the human body exposed to turbulent wind conditions. *Building and Environment, 169*, 106533.

Zhang, H. (2003). *Human thermal sensation and comfort in transient and non-uniform thermal environments*: University of California, Berkeley.

Zhang, Y., & Zhao, R. (2009). Relationship between thermal sensation and comfort in non-uniform and dynamic environments. *Building and Environment, 44*(7), 1386-1391.

Zhou, X., Lai, D., & Chen, Q. (2020). Thermal sensation model for driver in a passenger car with changing solar radiation. *Building and Environment, 183*, 107219.

Appendix

Step-change experiments were conducted in three adjacent areas of a campus to estimate the

stabilized time of globe temperature after transitioning from sunlight to shade and back to

sunlight (Figure A2). For each step-change experiment, the black ball thermometer used in this study was first exposed to one shade for 30 minutes, then quickly to sunlight for 30 minutes, and then quickly to the first shade for another 30 minutes. The measured globe temperature during experiments was displayed in Figure A1. According to the previous studies, the globe temperature lines in Figure A can be fitted to the exponential function (Eq. A).

$$y = Plateau + (y_0 - Plateau) * exp(-k * (x - x_0))$$

where y is the predicted value; x is the time corresponding to predicted y; x_0 is the time at which the change begins; y_0 is the y value up to time x_0; $Plateau$ is the y value at infinite times; k is the rate constant, expressed in reciprocal of the X axis time units.
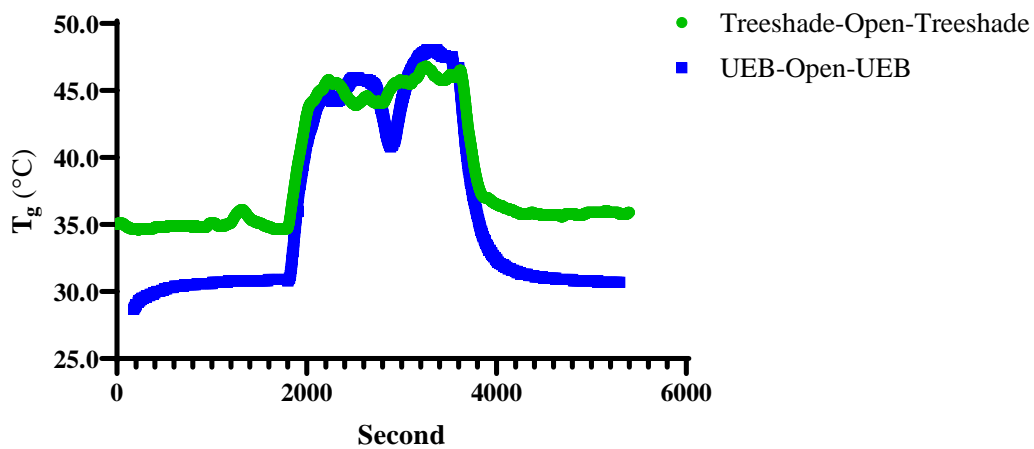

Figure A1. Variation of globe temperature from shade to sunlight and from sunlight to shade

a) Open garden   b) Large tree shade area   c) Area underneath an elevated building (UEB)

Figure A2. Sunlight and shade areas in a campus: a) an open garden; b) a large tree shade area; c) an area underneath an elevated building (UEB)

When y approached the plateau value, the stabilized times for globe temperature after upward and downward step changes were thus calculated by solving the x value with Eq. A. In this study, the stabilized times of T_g from tree-shade to sunlight and from UEB to sunlight are 2.5 minutes and 3.7 minutes, respectively. The stabilized times of T_g from sunlight to tree-shade and from sunlight to UEB are 2.7 minutes and 4.6 minutes, respectively. As indicated by Figure A1, it takes at least 2 minutes for the T_g to reach stability during the transition between sunlight and shade. Additionally, the greater the difference in T_g between the shade and sunlight, the longer the stabilized time is observed.